

The ($^3\text{He}, t\bar{p}$) reaction a means to study the microscopic structure of spin-isospin modes

M N Harakeh^a, H Akimune^b, I Daito^c, Y Fujita^d, M Fujiwara^c, M B Greenfield^e,
T Inomata^c, J Janecke^f, K Katori^g, S Nakayama^h, H Sakaiⁱ, Y Sakemi^c,
M Tanaka^j and M Yosoi^b

^aKVI, Zernikelaan 25, 9747 AA Groningen, The Netherlands

^bDepartment of Physics, Kyoto University, Kyoto 606, Japan

^cRCNP, Osaka University, Suita, Osaka 567, Japan

^dCollege of General Education, Osaka University, Osaka 560, Japan

^eNatural Science Division, ICU, Mitaka, Tokyo 181, Japan

^fDepartment of Physics, University of Michigan, Ann Arbor, MI 48109-1120, U S A

^gDepartment of Physics, Osaka University, Osaka 560, Japan

^hDepartment of Physics, Tokushima University, Tokushima, Japan

ⁱDepartment of Physics, University of Tokyo, Tokyo 113, Japan

^jKobe Tokiwa Jr College, Nagata 653, Japan

The microscopic structure of both the Gamow-Teller resonance (GTR) at $E_x = 15.6$ MeV and the spin-flip $\Delta L=1$ resonances at higher excitation energies in ^{208}Bi has been investigated by observing their direct proton decay to the $3p_{1/2}$, $2f_{5/2}$, $3p_{3/2}$, $1i_{13/2}$ and $2f_{7/2}$ neutron-hole states in ^{207}Pb , following their excitation via the $^{208}\text{Pb}(^3\text{He}, t)$ reaction at $E(^3\text{He}) = 450$ MeV. Decay protons were measured at backward angles in coincidence with tritons detected at very forward angles including $\theta = 0^\circ$. The total widths of the resonances as well as total and partial proton escape widths were determined and compared to theoretical estimates for the GTR. Using the same experimental set-up and conditions proton decay of the spin-flip $\Delta L=1$ resonances in ^{12}C was also measured.

1. INTRODUCTION

Thirty years have passed since the Gamow-Teller resonance (GTR) in nuclei was predicted to explain the retardation of Gamow-Teller transitions in β -decay compared to single-particle estimates [1,2]. Similarly, the spin-flip $\Delta L=1$ resonances were predicted to explain the strength of first-forbidden β -decay [3]. Although some evidence for the

GTR was found as early as 1975 [4], these charge-exchange collective excitations were not observed until the early eighties, when the study of the (p,n) reaction at intermediate bombarding energies ($100 \text{ MeV} < E_p < 500 \text{ MeV}$) became possible [5–7]. At these energies the (p,n) charge-exchange reaction preferentially excites spin-flip states [8–12]. Even though our knowledge of the systematics of the GT strength has improved considerably over the last decade, very little is known about the microscopic structure of either the GTR or the spin-flip $\Delta L=1$ resonances.

The microscopic structure of $\Delta T_Z=-1$ charge-exchange modes, which can be described as a coherent superposition of one-proton particle one-neutron hole configurations, can be investigated by studying their proton decay. The $({}^3\text{He}, t\bar{p})$ reaction has already been used at bombarding energies of $\simeq 30 \text{ MeV/u}$ to study the structure of the non-spin-flip isobaric analog resonance (IAR) in heavy nuclei [13–15] and the charge-exchange $\Delta L=1$ modes in light nuclei [16,17]. At intermediate energies ($\geq 100 \text{ MeV/u}$), the $({}^3\text{He}, t)$ reaction preferentially excites spin-isospin-flip modes [18,19]. This allows, in conjunction with proton decay, the study of the microscopic structure of charge-exchange spin-isospin modes. Such a study is not practical with the (p,n) reaction at intermediate energies because of the relatively low neutron detection efficiency, yielding very low coincidence rates in (p,n \bar{p}) experiments, and the relatively poor resolution achieved in detecting high energy neutrons ($E_n > 100 \text{ MeV}$). The typically poor neutron resolution, combined with the poor proton resolution resulting from the thick targets needed to obtain significant rates, yield typically more than 1 MeV total resolution for the final-state in the residual nucleus.

2. EXPERIMENTAL PROCEDURE AND DATA ANALYSIS

The experiments were performed at the Research Center for Nuclear Physics (RCNP) in Osaka. A 450 MeV ${}^3\text{He}^{++}$ beam extracted from the ring cyclotron was achromatically transported without any momentum defining slits onto a ${}^{208}\text{Pb}$ target of 5.2 mg/cm^2 thickness and of 99.86% isotopic enrichment. The ejectile tritons were detected in the spectrometer Grand Raiden [20], which has a K-value of 1400 MeV. The spectrometer was set at -0.3° with vertical and horizontal opening angles of 40 mrad each. The ${}^3\text{He}^{++}$ beam, having lower magnetic rigidity than the tritons, was fully intercepted by a specially designed Faraday cup in the first dipole magnet of the spectrometer. The ${}^3\text{He}^+$ particles, which are formed in the target and have about the same rigidity as the ejectile tritons, served as a calibration for the energy as well as for the scattering angle since they define the 0° spectrometer angle.

The ejectile tritons were detected with the focal-plane detection system which has two 2-dimensional position-sensitive multi-wire drift chambers (MWDC) backed by two ΔE -scintillation counters for particle identification. The horizontal and vertical scattering angles at the target were determined by ray-tracing techniques from the horizontal and vertical positions determined in the two position-sensitive detectors with uncertainties of less than 2 mrad and 10 mrad, respectively. Because of the characteristic angular distributions of the IAR, GTR and spin-flip $\Delta L=1$ resonances at angles near 0° , software cuts on the deduced scattering angles can be used in later off-line analyses to enhance

the relative contributions of these resonances in the spectra

Recently, the results for the GTR and IAR determined from our experiment have been published [21]. In this paper, it was shown that the characteristic angular distribution of $\Delta L=0$ transitions, which is sharply peaked at 0° , could be used to enhance their contributions in spectra relative to those of transitions of higher multipolarity and/or continuum background due to the quasi-free, charge-exchange process. Transitions of higher multipolarity have minima in their angular distributions at 0° , and the continuum due to the quasi-free charge-exchange process has a rather flat angular distribution near 0° . By studying the proton decay of the IAR and GTR in coincidence with tritons at these very forward angles, it was possible to determine their microscopic structure.

Figure 1 shows a singles spectrum where the triton scattering angles have been selected by ray-tracing to be centered at 1° . The software gates define horizontal and vertical opening angles of 14 mrad and 20 mrad, respectively. In this spectrum the $^3\text{He}^+$ peak is absent and, moreover, the contributions of the IAR and GTR are reduced in agreement with expectations based on their angular distributions [21]. However, the relative contributions from the $\Delta L=1$ spin-flip excitations (denoted by SDR) are enhanced. These resonances are superimposed on a non-resonant continuum background, which is assumed to result from quasi-free charge exchange. The figure displays the decomposition into the GTR, IAR, SDR and the non-resonant background. The continuum background (dash-dotted curve) has been calculated according to the prescription given in ref. [22]. The total width of the GTR was determined from fitting the GTR in the 0° spectrum [21] to be $\Gamma = 3.75 \pm 0.25$ MeV, and its excitation energy to be 15.63 ± 0.07 MeV. The total width of the SDR was determined from fitting the IAR, GTR and SDR in the 1° spectrum to be $\Gamma = 8.9 \pm 1.4$ MeV, and its excitation energy to be 21.01 ± 0.05 MeV. The parameters for the IAR, GTR and quasi-free continuum determined from this spectrum were in agreement with those determined from the 0° spectrum.

Protons from the decay of the IAR, GTR and SDR were measured in coincidence with tritons in eight solid-state detectors (SSD) arranged in two rings containing 4 SSD's each. The detectors in the outer ring were at $\theta = 132^\circ$, whereas those in the inner ring were at 157° . The SSD's in both rings were positioned at $\phi = 45^\circ, 135^\circ, 225^\circ$ and 315° . The detectors in the outer and inner rings were collimated to subtend solid angles of $\Delta\Omega = 57.8$ and 47.0 msr, respectively.

Time-of-flight spectra were generated for each SSD by starting and stopping a time-to-digital converter with timing signals from the focal-plane scintillator and the SSD, respectively. The time spectra (not shown here) had a ratio of prompt to random events of about 10. Two-dimensional scatter plots of proton energy measured in SSD versus excitation energy in ^{208}Bi were generated for prompt and random events by gating on prompt and random peaks in the time spectra. These 2-dimensional spectra were generated with gates on solid angles centered at 0° and 1° . A prompt 2-dimensional spectrum obtained for a gate on the solid angle centered at 0° was shown in Fig. 2a of ref. [21]. The loci for decay of the IAR, GTR and higher-lying resonances to the ground state (g.s.) and the low-lying neutron-hole states in ^{207}Pb ($1e_3p_{1/2}, 2f_{5/2}, 3p_{3/2}, 1i_{13/2}$,

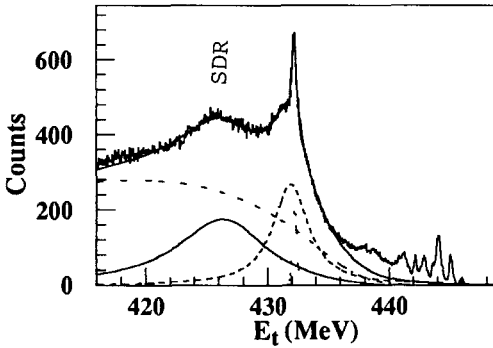


Figure 1 Triton energy spectrum from $^{208}\text{Pb}(^3\text{He},t)^{208}\text{Bi}$ obtained at $E(^3\text{He}) = 450$ MeV and at $\theta = 1^\circ$. The dashed, dotted, solid and dash-dotted lines represent fits obtained for GTR, IAR, spin-flip $\Delta L=1$ resonances (denoted by SDR) and non-resonant background, respectively.

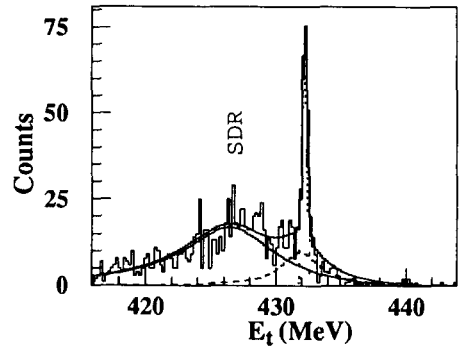


Figure 2 Triton energy spectrum at $\theta = 1^\circ$ gated on proton decay to neutron-hole states in ^{207}Pb after subtraction of random coincidences. The dashed, dotted, and solid lines represent the fits obtained for GTR, IAR, and SDR, respectively (see also Fig. 1).

$2f_{7/2}$) could be observed. The total resolution of the proton and triton sum energy was about 400 keV. This was not sufficient to completely resolve the decay to the 1st and 2nd excited states of ^{207}Pb . This could also be seen in the final-state spectrum obtained by projecting the loci on the excitation-energy axis of ^{207}Pb . This was shown in Fig. 2b of ref. [21], which was obtained by gating on the combined region of the GTR and IAR. The various peaks corresponding to decay to neutron-hole states in ^{207}Pb could be clearly observed. The branching ratios and partial proton escape widths could be determined from these spectra as discussed in ref. [21] and below.

A final-state spectrum obtained by gating on the solid angle centered at 1° and on the region of the SDR in the singles spectrum (not shown here) shows that the decay pattern for the SDR is different than that for the GTR. A relatively weaker population of the $3p_{1/2}$ and stronger populations of the $1i_{13/2}$ and $2f_{7/2}$ neutron-hole states are observed for the SDR.

A triton energy spectrum is shown in Figure 2. It was obtained by gating on decays to the neutron-hole states in ^{207}Pb and subtracting random coincidences. It is worth noting that in this spectrum the yield of the SDR relative to that of the GTR is even bigger than in the singles spectrum. Furthermore, the continuum due to quasi-free charge exchange, leading to emission of protons at very forward angles, is strongly suppressed (and therefore can be safely neglected) because coincidence is required with protons emitted at very backward angles. Thus the spectrum contains only the contributions of the IAR, GTR and SDR.

The parameters for the ^{12}C experiment were similar to the above-mentioned conditions for the ^{208}Pb experiment. A natural ^{12}C target with a thickness of 4.1 mg/cm^2

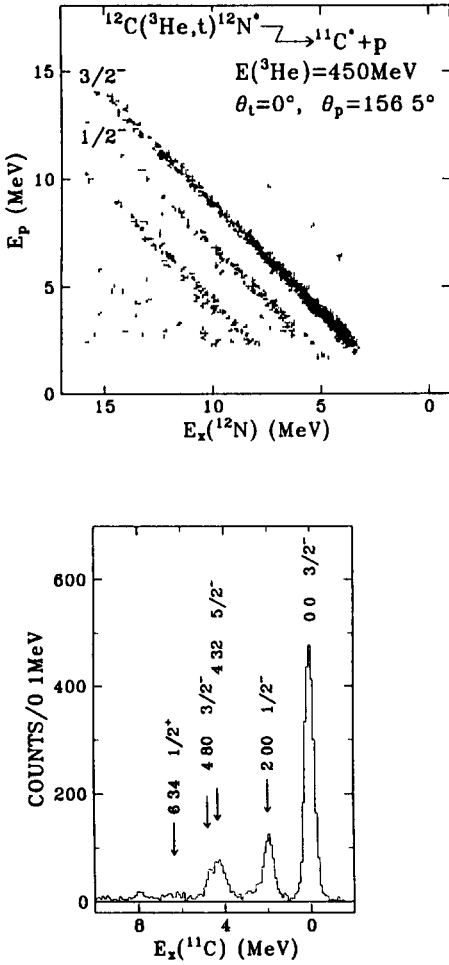


Figure 3 Top) two-dimensional scatter plot of proton energy versus triton energy [or excitation energy in ^{12}N] at $E(^3\text{He}) = 450 \text{ MeV}$ and at $\theta = 0^\circ$. The loci indicate proton decay to final states in ^{11}C . Bottom) the final-state spectrum of ^{11}C obtained from projecting loci of top figure onto the ^{11}C excitation-energy axis

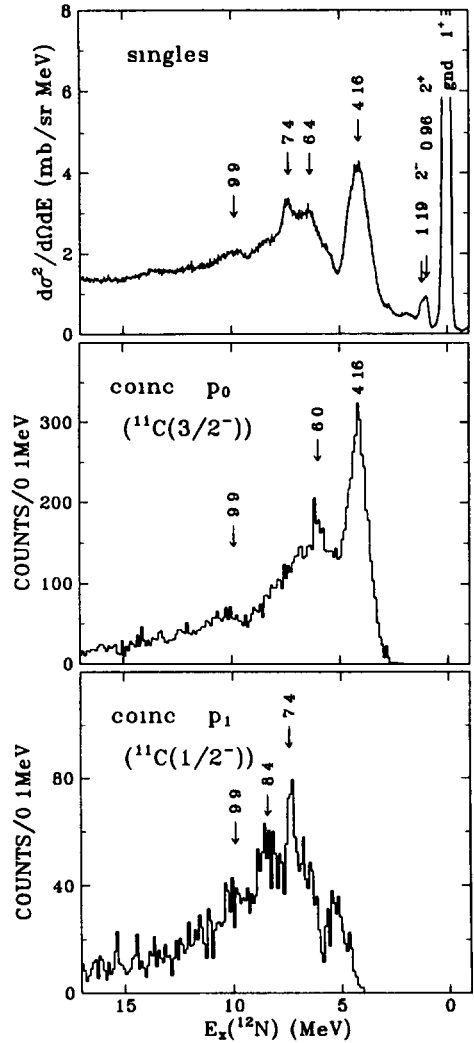


Figure 4 Triton energy spectra from $^{12}\text{C}(^3\text{He}, t)^{12}\text{N}$ obtained at $E(^3\text{He}) = 450 \text{ MeV}$ and at $\theta = 0^\circ$, singles spectrum (top), and spectra gated on proton decay to $3/2^-$ g.s (middle) and $1/2^-$ first-excited state (bottom) of ^{11}C after subtraction of random coincidences

was used. In Figure 3, a 2-dimensional spectrum (top) of proton energy versus triton energy (excitation energy in ^{12}N) is shown. Here, no cut on the solid angle was made to enhance $L=0$ transitions at very forward angles, as it is known that aside from the strongly excited 1^+ g.s. of ^{12}N little other spin-flip strength of positive parity is expected. Loci associated with decay to various states in ^{11}C can be clearly seen. The final-state spectrum obtained by projecting this 2-dimensional spectrum is shown in the bottom of Figure 3. The final states populated in ^{11}C are evident with the $3/2^-$ g.s. and $1/2^-$ first-excited state, which can be considered as $1p_{3/2}$ and $1p_{1/2}$ neutron-hole states, being the most prominent.

In the top of Figure 4, a $^{12}\text{C}(^3\text{He},t)^{12}\text{N}$ singles spectrum is shown which was obtained at $E(^3\text{He}) = 450$ MeV and at $\theta = 0^\circ$. In addition to the 1^+ g.s. of ^{12}N , structures are observed extending from 3 to 15 MeV excitation energy. Most of these structures may be associated with the spin-flip $\Delta L=1$ resonances, except possibly for some weak excitation of the non-spin-flip dipole resonance. In the middle and bottom of Figure 4, two spectra are shown which are gated on the peaks due to population of the $1p_{3/2}$ and $1p_{1/2}$ neutron-hole states in ^{11}C . Two features are worth mentioning. Firstly, the nuclear continuum due to knock-on charge exchange underlying the resonances is strongly suppressed in both coincidence spectra, as has been observed in the case of ^{208}Bi . Secondly, the resolved structures observed around 6.4 MeV and 7.4 MeV in the singles spectrum decay to different neutron-hole states indicating different microscopic structure.

3. RESULTS AND DISCUSSION

The total width of the IAR, GTR or SDR can be written as $\Gamma = \Gamma^{\uparrow} + \Gamma^{\downarrow}$, where Γ^{\uparrow} is the spreading width. In heavy nuclei, this leads to neutron decay. Statistical decay in the GTR region in ^{208}Bi favours neutron to proton decay by about three orders of magnitude as a consequence of the high Coulomb barrier. Γ^{\uparrow} is the escape width connected with the microscopic, one-proton particle, one-neutron hole structure of the GTR. This leads to direct proton decay to the neutron-hole states of ^{207}Pb and ^{11}C in the two reactions studied here. The escape width can thus be written as

$$\Gamma^{\uparrow} = \Gamma_p^{\uparrow} = \sum_i \Gamma_{p_i}^{\uparrow}, \quad (1)$$

where $\Gamma_{p_i}^{\uparrow}$ is the partial proton escape width associated with decay to the i th neutron-hole state of ^{207}Pb or ^{11}C . The ratio of Γ^{\uparrow} to the total width Γ can be obtained from the ratios of the coincidence double-differential cross sections to the singles cross section as

$$\frac{\Gamma_{p_i}^{\uparrow}}{\Gamma} = \frac{\int \frac{d^2\sigma_{p_i}}{d\Omega_i d\Omega_p} d\Omega_p}{\frac{d\sigma}{d\Omega_i}} = \frac{4\pi \frac{d^2\sigma_{p_i}}{d\Omega_i d\Omega_p}}{\frac{d\sigma}{d\Omega_i}} \quad (2)$$

Here, it is implicitly assumed that the double-differential and singles cross sections have been integrated over the excitation energy of the resonance. Since the decay of the GTR and IAR is expected to be isotropic, integrating the double-differential cross section yields a factor of 4π (right hand side of Eq. 2). In the case of the SDR one has to integrate over the observed angular correlation pattern.

3.1. ²⁰⁸Bi

The partial proton escape widths of the IAR and the GTR in ²⁰⁸Bi to the $3p_{1/2}$, $2f_{5/2}$, $3p_{3/2}$, and $2f_{7/2}$ neutron-hole states in ²⁰⁷Pb were determined from the measured branching ratios. The latter were determined from the peak areas of the IAR and GTR in spectra similar to that in Fig. 2 obtained by gating on the various final hole states in ²⁰⁷Pb as described above. For the GTR the proton escape widths are given in column 7 of Table 1. Since the resolution was not sufficient to separate the decay to the $2f_{5/2}$ and $3p_{3/2}$ neutron-hole states in ²⁰⁷Pb, the sum of the partial decay widths is given. This was also the case in the earlier experiment [13]. The present results for the IAR: 51.4 ± 5.6 keV ($\Gamma_{p_{1/2}}^\dagger$), 79.4 ± 9.4 keV ($\Gamma_{f_{5/2}}^\dagger + \Gamma_{p_{3/2}}^\dagger$) and 3.5 ± 1.6 keV ($\Gamma_{f_{7/2}}^\dagger$) are in very good agreement with the earlier experimental values [15] of 51.9 ± 1.6 keV, $(26.4 \pm 2.0 + 64.7 \pm 3.4)$ keV and 4.2 ± 0.6 keV, respectively. This nice agreement for the values determined for the IAR lends credence to the extracted values for the GTR which are in complete disagreement with the earlier experimental results listed in column 6. This confirms [23] that the earlier measurement [13] was not able to reliably measure the decay of the GTR due to the weak excitation of the GTR (no GTR bump could be observed) and to proton emission from competing reaction processes.

Table 1

Theoretical and experimental partial and total (escape) proton widths, $\Gamma_{p_i}^\dagger$ and $\Sigma_i \Gamma_{p_i}^\dagger$, in keV for the decay of the GTR in ²⁰⁸Bi into neutron-hole states in ²⁰⁷Pb

neutron-hole states in ²⁰⁷ Pb	E_x [keV]	theor ^{a)}	theor ^{b)}	theor ^{c)}	exp ^{d)}	exp ^{e)}
$3p_{1/2}^{-1}$	0	123.7	114.1	33	570 ± 70	58.4 ± 11.2
$2f_{5/2}^{-1}$	570	192.8	108.7	18	incl. in $p_{3/2}$	incl. in $p_{3/2}$
$3p_{3/2}^{-1}$	898	239.5	181.1	21	1130 ± 300	101.5 ± 15.6
$1i_{13/2}^{-1}$	1633	7.1	6.3	0.04	1780 ± 500	8.3 ± 9.2
$2f_{7/2}^{-1}$	2340	16.6	4.8	0.02	850 ± 300	15.6 ± 7.4
$1h_{9/2}^{-1}$	3413	7.9	2.9	0.26		
total		587.6	421.9	72	~ 4330	184 ± 49

^{a)} ref. [23] obtained with SGII interaction ^{b)} ref. [23] obtained with SIII interaction

^{c)} ref. [24] ^{d)} ref. [13], see also ref. [23] ^{e)} Present experimental results

Columns 3-5 display theoretical predictions. Columns 3 and 4 list the partial proton escape widths calculated by Van Giai et al. [23] in the Tamm-Dancoff approximation with explicit coupling to the continuum. These calculations were performed within the framework of a self-consistent microscopic theory where the single-particle states and the residual particle-hole interaction are derived from the same Skyrme force. Two different forces were considered, but only that used for the calculations of column 4 yielded an escape width for the IAR compatible with the experimental value. All theoretical results for the GTR, including those obtained by Muraviev and Urin [24] in RPA with coupling to the continuum (column 5) do not reproduce the data. Only the theoretically predicted

dominance of the decays into the three lowest single-neutron hole states is confirmed by the new data. However, it is worth noting that recent calculations both by Udagawa et al [25] and Van Giai et al [26] showed respectively good to reasonable agreement with the experimental results.

For the decay of the SDR in ^{208}Bi , the partial proton escape widths to the various neutron-hole states in ^{207}Pb have not been determined nor have the various spin components (2^- , 1^- and 0^-) of the SDR been disentangled using their angular correlation patterns. However, one can infer from the final-state spectra (not shown here) that the population pattern of the various neutron-hole states is different for the SDR than that for the GTR, in that the $1_{i13/2}$ and $2_{f7/2}$ are more strongly and the $3_{p1/2}$ more weakly populated. Furthermore, the total proton decay branching ratio has been determined from the coincidence spectra to be $14.6 \pm 1.3\%$. If assumed to be due to decay of one single resonance with a width of 8.9 MeV , this would lead to a total proton escape width of $1.30 \pm 0.23\text{ MeV}$. However, the SDR bump consists of three spin components, 1^- , 2^- , 1^- and 0^- . Even if one considers that the total proton escape width determined above should be divided among these three components, the resulting proton escape width per component is still considerably larger than for the GTR. This has to do with the increase of the proton energy available above the Coulomb barrier and also the average decrease of the angular-momentum barrier for the decay protons as compared to the GTR. Indications also appear for proton decay to the $1h_{9/2}$ broad neutron deep-hole state in ^{207}Pb .

3.2. ^{12}N

The angular distributions of the various resonance structures between 3 and 15 MeV in ^{12}N in the very forward angular region (0° - 1.5°) indicate predominantly $L=1$ transfer, implying the excitation of the spin-flip $\Delta L=1$ (2^- , 1^- and 0^-) resonances in ^{12}N . In addition, the non-spin-flip 1^- charge-exchange dipole resonance may also be weakly excited at this ^3He bombarding energy.

Comparing the ^{12}N singles spectrum with the coincidence spectra gated with decay to the $1p_{3/2}$ and $1p_{1/2}$ neutron-hole states in ^{11}C (shown in Fig. 4) one can clearly observe different population of these hole states from the two resolved structures at $\simeq 6.4\text{ MeV}$ and 7.4 MeV excitation energy in ^{12}N . This clearly indicates different microscopic structures for these two resonances. It is tempting to assign predominantly $J^\pi=2^-$ to the structure at 6.4 MeV . This would be consistent with its observed steep angular correlation for proton decay to the $3/2^-$ g.s. of ^{11}C , which is very similar to that of the known 2^- resonance at about 4.2 MeV excitation energy. Evidence for a 2^- assignment from ($\vec{d}, ^2\text{He}$) and ($^{12}\text{C}, ^{12}\text{B}$) measurements made at RIKEN for a resonance around this energy were presented at this conference. The higher resonance at about 7.4 MeV would most probably have $J^\pi=1^-$ because of its favored decay to the $1/2^-$ first-excited state of ^{11}C , and because of its less steep angular correlation pattern for proton decay to the $3/2^-$ g.s. of ^{11}C .

The angular correlation for proton decay to the $3/2^-$ g.s. of ^{11}C of the resonance structure at around 10 MeV is within the uncertainties isotropic, which is consistent with a 0^- spin assignment for this structure. Although this may not be a sufficient

condition to make a definite spin assignment, theoretical calculations [27] predict 0^- strength at about this energy. A detailed comparison with angular correlations based on microscopic DWBA calculations is necessary before a more definite assignment can be made. It is interesting to note, however, that this is the only structure observed to decay to the $1/2^+$ state at 6.34 MeV in ^{11}C , which may be connected with the microscopic structure of the 0^- resonance.

REFERENCES

- 1 K Ikeda, S Fujii and J I Fujita, Phys Lett 3 (1963) 271
- 2 J I Fujita and K Ikeda, Nucl Phys 67 (1965) 145
- 3 H Ejiri, K Ikeda and J I Fujita, Phys Rev 176 (1968) 1277
- 4 R R Doering et al, Phys Rev Lett 35 (1975) 1691
- 5 D E Bannum et al, Phys Rev Lett 44 (1980) 1751
- 6 C D Goodman et al, Phys Rev Lett 44 (1980) 1755
- 7 D J Horen et al, Phys Lett B95 (1980) 27
- 8 F Petrovich and W G Love, Nucl Phys A354 (1981) 499c
- 9 N S P King et al, Phys Lett B175 (1986) 279
- 10 W P Alford et al, Phys Lett B179 (1986) 20
- 11 T N Taddeucci et al, Nucl Phys A469 (1987) 125
- 12 B S Flanders et al, Phys Rev C 40 (1989) 1985
- 13 C Gaarde et al, Phys Rev Lett 46 (1981) 902
- 14 H J Hofmann et al, Nucl Phys A433 (1985) 181, and references therein
- 15 S Y van der Werf, M N Harakeh and E N M Qunt, Phys Lett B216 (1989) 15, and references therein
- 16 W A Sterrenburg et al, Nucl Phys A405 (1983) 109
- 17 W A Sterrenburg et al, Nucl Phys A420 (1984) 257
- 18 C Ellegaard et al, Phys Rev Lett 50 (1983) 1745
- 19 I Bergqvist et al, Nucl Phys A469 (1987) 669
- 20 M Fujiwara et al, Nucl Instr Meth Phys Res A, (to be published)
- 21 H Akimune et al, Phys Lett B323 (1994) 107
- 22 J Janecke et al, Phys Rev C 48 (1993) 2828, and references therein
- 23 N Van Giai et al, Phys Lett B233 (1989) 1
- 24 S E Muraviev and M G Urin, Nucl Phys A (in print)
- 25 T Udagawa et al, elsewhere in these proceedings
- 26 N Van Giai et al, elsewhere in these proceedings
- 27 V Gillet and N Vinh Mau, Nucl Phys 54 (1964) 321